Laser Heating Nanoelectrospray Emitters for Fast Protein Melting Measurements with Mass Spectrometry

Jacob S. Jordan and Evan R. Williams*

Department of Chemistry, University of California, Berkeley, CA 94720 USA

*To whom correspondence should be addressed

e-mail: erw@berkeley.edu

Abstract

Temperature-controlled nanoelectrospray ionization has been used to measure heat-induced conformational changes of biomolecules by mass spectrometry, but long thermal equilibration times associated with heating or cooling an entire emitter limits how fast these data can be acquired. Here, the tip of a borosilicate electrospray emitter is heated using 10.6 μm light from an unfocused CO_2 laser. At 1.2 W, the solution inside the emitter tip can be heated from room temperature to a steady state temperature of 78.2 ± 2.5 °C in less than 0.5 s and cools from 82.6 ± 0.6 °C back to room temperature within 4 s. The time required to establish a steady state temperature is more than 100 fold faster than that required for a resistively heated emitter due to the low thermal mass. Protein unfolding curves measured as a function of laser power can be acquired in ~40 s compared to a resistively heated apparatus that required ~21 min. to acquire similar data. Laser power is calibrated to temperature by comparisons of the average charge state of the protein cytochrome *c* measured with laser heating and with resistive heating. This laser heating method is applied to a three-component protein mixture to demonstrate the ability to rapidly acquire melting temperatures of proteins in mixtures. The ability to rapidly assess the thermal stabilities of multiple proteins simultaneously shows significant promise for coupling temperature-controlled ESI to separations techniques, providing a high-throughput method for determining the effects of solution composition, drug-binding, or sequence mutations on protein thermal stability.

Introduction

The thermodynamic stabilities of the native states of proteins and macromolecular complexes are fundamental properties that influence conformational diversity, solubility, and function. The stability of a protein native state can be measured using a variety of different methods, including chemically induced or thermally induced protein unfolding.[1] Temperature-induced unfolding data can be used to obtain a melting temperature (T_m) and other useful thermochemical information.[2] Thermal stabilities depend on solution composition and pH,[3] sequence mutations[4,5] and ligand/drug-binding,[3,6] making T_m values a useful metric when studying the stabilizing effect of formulation buffers[3] or identifying small molecule ligand binding in drug development workflows.[7] A variety of standard techniques are used to measure protein melting temperatures, including circular dichroism (CD) spectroscopy,[2,8] fluorescence/UV-Vis spectrophotometry[9,10] and differential scanning calorimetry (DSC).[11,12] These techniques generally require purified protein samples in order to avoid overlapping signals or transitions that lead to uncertainties in measured T_m values. Mass spectrometry (MS) has also been used to measure protein melting temperatures and has the advantage that purified samples are not required if proteins have different masses.[13,14] MS-based methods of determining T_m values also have the advantage of high sensitivity with little sample required, and changes in protein conformation, including folding/unfolding intermediate structures that are kinetically trapped during the ionization process,[15–17] can be identified based on either the abundance of each charge state[18–20] or by using ion mobility spectrometry.[16,20–23]

Several different variable-temperature electrospray ionization (vT-ESI) sources have been developed to change solution temperature during electrospray.[8] Resistively heated devices are most common, but heating or cooling has also been done with Peltier devices.[8] vT-ESI has

been used to measure protein,[8,12,19–21,24–27] protein complex,[22,23,25,28–30] and DNA complex unfolding pathways and kinetics,[6,31] determine thermochemical values of protein[18,23,32–34] and peptide stability,[35] and to determine binding energetics of small molecule ligands.[32,36,37] Recently, El-Baba *et al.* determined T_m values of seven proteins from a mixture of ribosomal proteins using vT-ESI, illustrating the advantage of this technique for multiplexed measurements.[19]

Heating/cooling devices differ in the accessible temperature ranges and the rates at which the temperature can be changed.[8] However, a common characteristic of these devices is a relatively large thermal mass associated with heating the entire apparatus. A high thermal mass necessitates long thermal equilibration times of between 1 – 3 minutes before measuring mass spectra at each temperature.[8,12,18,20,24,28,36,37] Cooling the source between melting replicates can take >10 minutes, significantly reducing the throughput of this technique.

One alternative technique to measure protein melting by mass spectrometry is "laser-spray" in which a laser is used to heat the analyte solution. Initial laser-spray experiments by Hiraoka and coworkers using a 10.6 μm CO_2 laser were performed with the laser beam pointed down the barrel (coaxial orientation) of a stainless steel capillary with an inner diameter of 100 μm.[38–42] With a laser power of 0 W and 1.6 W, the relative abundance of the folded forms of cytochrome *c* at pH 3.5, determined by a change in the average charge state, was ~81 % and ~15 %, respectively.[38] These data fit well to a sigmoidal curve from which a melting power was determined from the inflection point of the curve.[38] Laser-spray has been utilized to study the effects of laser power on stabilities of proteins,[43] protein-DNA,[44] and DNA-drug complexes.[45]

A focused 10.6 μm laser has also been used to heat nanodroplets produced from electrospray emitters.[15,21] El-Baba *et al.* reported an increase in the weighted average charge state

of ubiquitin with increasing laser power, similar to that reported for vT-ESI experiments, indicating that this technique is also applicable for the study of protein thermal denaturation.[15] Changing the diameter of the tip of the electrospray emitter and hence the initial droplet size distribution produced by electrospray[46–48] resulted in a different extent of unfolding. These experiments indicate that thermally induced protein unfolding kinetics and structural intermediates can be investigated by producing droplets that have different initial sizes and hence lifetimes. Woodall *et al.* reported different extents of myoglobin unfolding by vT-ESI and nanodroplet heating with this same apparatus.[21] The weighted average charge state of holo-myoglobin increased by +4.0 charges during vT-ESI experiments at pH 9, but only by +1.5 and +2.5 from heating droplets produced by emitters with 4 μm and 24 μm diameter tips, respectively. Because equilibration times in vT-ESI experiments are typically on the order of one minute or more when the temperature of a solution is changed, conformational changes that occur likely reflect equilibrium conditions. In contrast, the time scale for protein folding/unfolding in droplets depends on the lifetime of the droplet[48,49] that can be readily varied between ~1 μs to ~50 μs.[47,49]

Here, a laser heated electrospray ionization (LH-ESI) source that uses a 10.6 μm CO_2 laser to heat only the tip of a borosilicate nanoelectrospray ionization emitter was constructed. Strong absorption of 10.6 μm light by borosilicate enables low laser fluences to be used to reach solution temperatures >80 °C. By rapidly changing laser power, protein melting curves can be acquired in less than 45 s. This method shows significant potential for rapidly determining protein melting temperatures by mass spectrometry, including the ability to acquire data on a separations time scale.

Materials and Methods

A laser-heated ESI (LH-ESI) source (Figure 1) was constructed by aligning the beam of a Synrad F48-2 10.6 μm CO_2 laser (Synrad Corporation, Mukilteo, WA) perpendicular to the inlet of an Orbitrap Elite mass spectrometer (ThermoFisher Corporation, Waltham, MA). Borosilicate emitters were aligned with the laser beam and the tip length that was irradiated with the laser was controlled by a beam block that prevents the rest of the capillary from being heated (Figure 1, inset). An IR power meter head (Ophir-Spiricon, North Logan, UT) after the capillary was used to measure laser power in real time. An Arduino microcontroller (Uno R3, Somerville, MA) with an Adafruit MCP4725 DAC (New York, NY) was programmed to read and change the laser power during the experiment via Arduino and Python code. Emitters were positioned in the beam path using a 3-axis stage using both a Dino-Lite digital microscope to visualize the distance from the MS inlet to the emitter and a 633 nm Helium-Neon laser (ThorLabs, Newton, NJ) that was co-aligned with the CO_2 laser beam. The variability between replicates reflects variations in tip morphology and tip positioning in addition to other variations typical in nano-ESI-MS experiments. An electrospray voltage (1.0 – 1.5 kV) was supplied via a 0.127 mm diameter platinum wire inserted into the back of the capillary and in contact with the solution.

Borosilicate nanoelectrospray capillaries (1.0 mm outer diameter, 0.78 mm inner diameter, Sutter Instrument, Novato, CA) were pulled to an inner diameter of ~1.3 ± 0.1 μm and a taper length of 3.5 ± 0.1 mm using a Sutter Instrument P-87 capillary puller.[50] Emitters were periodically imaged using a Hitachi TM-1000 scanning electron microscope (Tokyo, Japan) at the University of California, Berkeley Electron Microscopy Lab.

For calibration purposes, a vT-ESI source similar to that described by Sterling *et al.* was constructed.[51] In brief, the source consists of an aluminum cylinder wrapped in resistive heating

wire. The temperature of the apparatus was measured using a J-type thermocouple positioned within the metal heating jacket and was controlled using an Omega CNi3222 temperature controller (Stamford, CT). Borosilicate capillaries were inserted through the aluminum cylinder until the emitter tip was at the end of the heating jacket. A thermocouple placed inside the borosilicate capillary was used to confirm that the thermocouple in the heating jacket reflected the temperature inside the capillary. The temperature of the device was allowed to equilibrate for ~70 s at each temperature prior to starting electrospray and ~6 mass spectra (~3 s) were averaged at each temperature during analysis.

For cytochrome *c* (cyt *c*) melting experiments, 10 μM equine cyt *c* was prepared in 20 mM ammonium acetate at pH 6.8. The laser power was increased from 0 W to ~1.3 W in increments of ~75 mW and ~6 spectra were averaged at each laser power (~3 s). The instrument resolution was set to 60000 with a maximum injection time of 10 ms, resulting in a mass spectrum acquisition rate of ~0.42 s. To determine the effect of emitter position on protein melting, the tip position was adjusted in all three axes using micron adjusts and spectra were acquired for 15 s at a constant laser power of ~600 mW. To achieve higher spectral acquisition rates in experiments where the rate of heating was measured, the instrument resolution was set to 15000, resulting in a mass spectrum acquisition rate of 0.25 s. Solutions containing a mixture of cyt *c*, equine heart myoglobin, and pseudo-wildtype barstar were prepared (3 μM each) in 20 mM ammonium acetate (pH 6.8). Cyt *c* and equine heart myoglobin were obtained from Sigma-Aldrich (Burlington, MA) and were used without further purification. Pseudo-wildtype barstar (C40/82 replaced by Ala) was obtained as previously described.[52]

Results and Discussion

Performance of Laser Heated NanoESI. Borosilicate capillaries often used in nanoESI have tip diameters that are typically in the low tens of micron range, although emitter tips with diameters of a few microns or lower can be advantageous for native MS measurements.[53,54] Borosilicate absorbs strongly at the 10.6 μm output of a CO_2 laser and the emitter tips have low thermal mass. Because laser power can be changed quickly, laser irradiation of just the emitter tip should lead to a rapid change in solution temperature, which can induce protein unfolding. An apparatus was constructed (Figure 1) to accurately position an emitter tip in the beam of a CO_2 laser (~3.5 mm beam diameter) and to block laser light so that only the tip of the emitter is exposed to the laser beam. Factors that affect the heating of solution in an emitter tip with this apparatus were investigated using a solution of 10 μM cytochrome *c* (cyt *c*) in 20 mM ammonium acetate. The weighted average charge state was used as an indicator of protein conformation in solution.

The emitter position was adjusted along three axes at a constant laser power (~600 mW) in order to determine how the position affects solution heating during laser irradiation. An emitter tip was centered ~2.5 mm distant to the heated metal capillary interface of the mass spectrometer, and the final ~0.5 mm of the emitter tip was exposed to the laser beam. Under these conditions, the weighted average charge state for cyt *c* was 9.94 ± 0.08 (Figure S1), corresponding to half of the protein in an unfolded form, compared to a value of 6.93 ± 0.02 when the emitter tip was not heated and the protein is fully folded.

With the emitter tip behind the beam block, there is no change in the average charge state of cyt *c* when the laser is on, even though nanodroplets formed by ESI pass through the ~600 mW laser beam before entering the mass spectrometer. This indicates that the nanodroplets are not significantly heated by the relatively low power of the unfocused laser beam, consistent with

earlier CO_2 laser heated droplet experiments that required higher laser power (up to 17 W) focused to a 500 μm spot size to induce protein unfolding.[15,21] Exposing the emitter tip to more laser irradiation by positioning it ~1.5 mm in front of the beam block increased the weighted average charge state of cyt *c* to 10.8 ± 0.1, which is significantly higher than the value of 9.94 ± 0.08 when the tip is positioned only ~0.5 mm in front of the beam block. This indicates that exposing more of the emitter tip to the laser beam leads to higher solution temperature, either as a result of greater thickness of the borosilicate material further from the emitter tip leading to more absorption of the laser light or relatively lower conductive heat loss either to the surrounding air or to the rest of the capillary.

Adjustment of the emitter tip position along the *y*-axis (up or down with respect to the laser beam) also affects the average charge state of cyt *c* ions (Figure S1). The weighted average charge state varied from 7.06 ± 0.09 to 9.94 ± 0.08 over the distance ± 1 mm from the center. In contrast, adjustment of the emitter position ~0.5 mm left or right along the *z*-axis (axis of beam propagation) resulted in an average change in the weighted average charge state of only 0.2 (Figure S1), consistent with the low divergence of the laser along the direction of propagation. The ion signal is similar at each emitter position, indicating the differences in the observed charge-state distribution are due to different extents of heating and not differences in ion collection efficiency. These results indicate that careful positioning of the emitter with respect to the length exposed to laser light and the centering of the emitter within the beam is necessary in order to obtain reproducible heating of the solution inside the emitter. In subsequent experiments, the emitter was positioned so that the +12 charge state of cyt *c* was at ~50% relative abundance to the +7 charge state at ~600 mW of laser power to ensure reproducible tip positioning.

Rate of Laser Heating and Conductive Heat Loss. The rate of solution heating and cooling with LH-ESI was compared to that obtained using a resistively heated ESI emitter based on an earlier design.[51] With the latter device, changing the temperature of 20 μL of solution from ~79.5 °C to ~85 °C requires ~70 s (Figure S2). This time is consistent with that reported for other devices where thermal equilibration times at each temperature of ~1 – 3 minutes have been reported.[8,12,18,20,24,28,36,37]

In contrast, the solution inside the tip of an electrospray emitter can be rapidly heated using a laser. Changing the laser power from 0.0 W (ambient temperature) to ~1.2 W results in a change in the average charge state of cyt *c* from 6.92 ± 0.03 to 10.3 ± 0.3 within the duration of two mass spectral acquisitions (~0.5 s) and remains nearly the same with continued irradiation, indicating that the solution temperature has reached a steady state in less than 0.5 s (Figure 2, right axis). An exponential fit to the data results in a time constant of 0.11 s^{-1}. These data indicate that the time required to establish a steady state temperature upon heating an emitter tip with a laser (<0.5 s) is more than a factor of 100 less than that required for conventional vT-ESI sources. The rapid heating and thermal steady state is likely due to the small volume of liquid that is heated inside the emitter tip and the low thermal mass of the emitter tip.

The absorption coefficient at 10.6 μm for Corning 7740 borosilicate glass used in Sutter Instrument capillaries has been reported to be 4893 cm^{-1} and 7812 cm^{-1} by the KBr pellet technique and the reflection method,[55] respectively, compared to a value of ~832 cm^{-1} for water.[31] Thus, the capillary absorbs light at a rate that is ~6 – 9 times greater than the aqueous solution itself. This indicates that the temperature of the borosilicate glass is higher than that of the solution, but the fast thermal steady state in solution indicates that heat conduction from the capillary to the aqueous solution occurs rapidly.

To investigate how rapidly the solution inside the electrospray emitter cools upon turning off the laser, the same cyt *c* solution was irradiated at 1.3 W, the highest laser power used in these experiments. The average charge state was 10.92 ± 0.03 prior to turning off the laser, upon which time, the average charge state decreased over the course of four seconds and returned to a steady state value of 6.95 ± 0.01, the same as that prior to turning on the laser (6.92 ± 0.03) (Figure 2, right axis). These data show that conductive heat loss from the emitter to the surrounding air is rapid and indicates that temperature melting data can be cycled from high to low temperature within four seconds.

Rapid Protein Melting Measurements. The performance of the LH-ESI apparatus for rapid protein melting measurements was evaluated by acquiring mass spectra of a solution of 10 μM cyt *c* in 20 mM ammonium acetate (pH 6.8) as a function of laser power from 0 W to 1.3 W. Upon increasing the laser power from 0 W to 1.3 W, the weighted average charge state of cyt *c* ions increased from ~6.93 ± 0.02 to ~10.85 ± 0.03, indicating that the protein population transitions from entirely folded to ~77% unfolded (Figure 3, red curve). The average charge state as a function of laser power was fit to a 7-parameter sigmoidal function. This resulted in a melting power, P_m, of ~0.60 ± 0.02 W obtained from three replicate measurements in which different electrospray emitters were used. The deviation in P_m between replicates is likely due to minor differences in positioning each emitter. Each of the replicate melting curves has the same shape, so a small linear power adjustment (<5%) can be done to make the melting powers for each curve match. This reduces the effects of minor differences in emitter positioning. The resulting P_m after these adjustments was 0.599 ± 0.001 W.

Protein thermal denaturation has also been observed by "laser-spray" ESI and by heating nanodroplets using a focused 10.6 μm laser beam. Shi *et al.* observed denaturation of cyt *c* in 1

mM ammonium acetate during laser-spray ESI using a 100 μm diameter stainless steel emitter at similar laser powers to those reported here.[38] At laser powers >1.6 W, cyt *c* dimers were observed. The authors proposed that the dimer signal is due to solvent evaporation at higher temperatures that increased concentration of cyt *c* at the emitter tip. Cyt *c* dimer signal is not observed at any laser power in the LH-ESI experiments reported here, likely due to the relatively small surface area exposed at the end of the borosilicate emitters, which reduces solvent evaporation. Nanodroplet heating experiments by El-Baba *et al*. required much higher laser fluences (up to 17 W and a beam focus of 500 μm) due to the low absorbance cross-section of water at this wavelength.[15] In our LH-ESI experiments, an unfocused laser at a power of only 1.3 W was sufficient to achieve complete melting of cyt *c* (T_m = 73.5 ± 0.5 °C) owing to the high absorbance of borosilicate at this wavelength. At laser powers between 6 – 10 W, significantly higher than those used for LH-ESI experiments, emitters were observed to melt, disrupting the electrospray process.

In a separate experiment, the laser beam was focused to ~1 mm diameter in front of the emitter tip using a 50 mm focal length lens. There is no change in the average charge state when the laser power is changed from 0 W to ~17 W (Figure 3, left inset). These results indicate that a higher power is required to heat the nanodroplets to sufficient temperatures to initiate cyt *c* unfolding and that droplet heating is negligible in the LH-ESI experiments. The lower power required to achieve complete melting of a relatively stable protein with LH-ESI is an advantage of heating the emitter directly compared to heating the nanodroplets at 10.6 μm.

Because the solution temperature in LH-ESI experiments reaches a steady state in <0.5 s upon a large change in laser power, the laser power can be varied rapidly in order to measure protein melting curves. The LH-ESI melting curve of cyt *c* shown in Figure 3 required only ~40

s of total acquisition time per replicate to obtain. The acquisition speed is ultimately limited by the signal-to-noise ratio obtained in the mass spectral data. These spectra have high S/N (Figure 3, left inset) indicating the potential for these data to be acquired more quickly.

In contrast, the resistively heated vT-ESI source required much longer time to acquire temperature melts owing to the time necessary to establish a steady state at each set temperature. Data obtained for cyt *c* from ~27 °C to ~90 °C is shown in Figure 3. Over this temperature range, the average charge state increased from ~7.00 ± 0.03 to ~11.1 ± 0.3 (Figure 3, blue curve). An average charge state of 11.1 at ~90 °C from vT-ESI is similar to the value of 10.9 obtained at 1.3 W from LH-ESI, indicating that a similar temperature is achieved between these two methods. Increasing the solution temperature beyond ~90 °C resulted in a loss of signal due to bubble formation in the emitter tip that stopped the spray. A sigmoidal fit to the data results in a T_m of 73.5 ± 0.5 °C, matching well with prior reported values.[25,56] Because a minimum of 70 s between temperature points was needed to ensure a steady state temperature, the vT-ESI experiments required approximately 21 minutes per replicate. Consequently, >1 hour was required to acquire the three replicates shown in Figure 3 using vT-ESI. These results indicate that protein thermal denaturation data can be acquired 30 times faster with LH-ESI than resistively heated vT-ESI. However, the laser-heated method requires calibration in order to convert laser power to solution temperature.

Calibrating Laser Power to Solution Temperature. Melting powers determined from LH-ESI can be converted into melting temperatures by comparison to vT-ESI data. The change in the average charge state of cyt *c* for both LH-ESI and vT-ESI experiments was normalized between 0 and 1 (Δq). The Δq value at each laser power from LH-ESI was compared to that at each temperature from vT-ESI to determine an effective solution temperature within the tip

during laser irradiation. When the Δq values are equal between these two experiments, then the temperatures within the tip should be the same. By finding each point where the normalized values are equal, a calibration curve was constructed to convert the measured laser power to temperature (Figure S3).

The laser power to temperature conversion makes it possible to determine how the solution *temperature* changes after the laser is turned on or off from the change in the average charge state as a function of time. Upon turning the laser power on to ~1.2 W, the average charge state of cyt *c* increases from the ambient temperature value of 6.92 ± 0.03 to 10.33 ± 0.32 in <0.5 s, corresponding to a solution temperature of ~78.2 ± 2.5 °C (Figure 2, left axis; steady state temperature of ~77.4 ± 1.4 °C at later times). The data were fit to an exponential function with a time constant of 0.07 ± 0.01 s^{-1}.

A laser power of 1.3 W results in an average charge state of cyt *c* of 10.92 ± 0.03 corresponding to a solution temperature of 82.6 ± 0.6 °C (Figure 2, left axis). Upon turning off the laser, the average charge state of cyt *c* decreased to 7.30 ± 0.04 within the acquisition time of a single mass spectrum (~0.42 s), corresponding to a temperature of ~56 ± 3 °C. The solution temperature returns to ~28.5 °C (ambient temperature, the ESI emitter is close to the heated electrospray interface of the mass spectrometer) within four seconds. The data were fit to a single exponential function with a decay rate of 1.0 ± 0.1 s^{-1}. These experiments confirm that the solution temperature inside the ESI emitter rapidly reaches a steady state upon turning on the laser, cools quickly once the laser is turned off and that measurements in LH-ESI can be made within 0.5 s provided that the temperature is not reduced by more than 25 °C within this time. In contrast, emitters heated with the vT-ESI source required ~13 minutes on average to cool to room temperature after acquisition of a single melting curve as a result of the larger thermal mass

associated with the aluminum heating jacket. Although this time could be reduced by actively cooling the emitters, either using Peltier devices or forced air-cooling for example, the cooling time between replicates poses a significant barrier to making vT-ESI techniques high-throughput.

This laser power to temperature conversion can be used to determine the T_m values of other proteins that have not been characterized by vT-ESI. However, positioning of the tip is critical (Figure S1) in order for this same calibration data to be used. To reduce the uncertainties in tip positioning, cyt *c* was used as an internal calibrant of temperature to more accurately measure the melting temperatures of other proteins in a solution.

Determining T_m Values with LH-ESI. In order to investigate the accuracy of LH-ESI for measuring T_m values of other proteins using cyt *c* as an internal calibrant, LH-ESI and vT-ESI data were obtained for a solution containing cyt *c*, equine heart myoglobin, and pseudo-wild type barstar (Ψbar*) at 3 μM each (Figure 4). The weighted average charge of cyt *c* increases from 6.9 ± 0.1 to 11.0 ± 1.0 upon an increase in temperature from ~29 °C to ~90 °C, comparable to the change from 7.05 ± 0.02 to 10.28 ± 0.09 upon increasing the laser power from 0 W to ~900 mW. Further increases in laser power resulted in unstable spray. The population abundance of apo-myoglobin ions (myoglobin that has lost a noncovalently bound heme) increased from 1.0 % ± 1.0 % to 100 % ± 0 % and 1.6 % ± 2.8% to 98.3 % ± 0.3 % across the same ranges of temperature and laser power, respectively. The protein Ψbar* undergoes a much smaller change in the weighted average charge state from 5.4 ± 0.1 to 6.4 ± 0.1 between ~29 °C and ~68 °C in vT-ESI experiments. Above 68 °C, Ψbar* ions are not observed in the vT-ESI mass spectra. However, during LH-ESI Ψbar* ions are observed at the highest laser powers and the weighted average charge state increases from 5.4 ± 0.1 at 0 W to 6.6 ± 0.1 at ~900 mW. The observation of Ψbar* ions at a higher temperature with LH-ESI may be related to the different experimental

time scales. Formation of nonspecific aggregates of denatured Ψbar* may occur during the long thermal equilibration times in vT-ESI, whereas aggregates may not form as quickly during LH-ESI due to the rapid measurement (<45 s). LH-ESI data for Ψbar* at low laser powers has significant scatter, which may be related to variations in laser power near the threshold for lasing. These data highlight an advantage of MS-based measurements of thermal stability – the capacity to measure the thermal denaturation of multiple proteins from the same solution simultaneously.

The Δq values were determined from these data and a temperature calibration using cyt *c* was applied to the LH-ESI data to generate the melting curves shown in Figure 4. A sigmoidal fit to the vT-ESI data resulted in T_m values for cyt *c*, myoglobin, and Ψbar* of 76.3 ± 4.2 °C, 71.6 ± 0.5 °C, and 58.2 ± 1.5 °C, respectively (Figure 4, dashed lines). T_m values determined from temperature-recalibrated LH-ESI measurements were 73.1 ± 1.2 °C, 71.5 ± 0.9 °C, and 63.1 ± 4.7 °C for cyt *c*, myoglobin, and Ψbar*, respectively, which agree well with values obtained by vT-ESI (Figure 4, solid lines).

The temperature calibration is most sensitive when there is a large change in average charge state with increasing temperature. The change in average charge state of cyt *c* is small at low temperature leading to greater uncertainty in the low temperature region. The larger difference in T_m values for Ψbar* obtained with the two methods may in part be attributed to this effect. More reproducible positioning of the emitter tips and calibrating the laser power using multiple proteins that have different T_m values should increase the accuracy and precision of the LH-ESI method. Combined, these experiments demonstrate the potential of LH-ESI for the high-throughput measurement of protein thermal stabilities by nESI-MS and elucidate the practical considerations for performing LH-ESI measurements of protein melting temperatures.

Conclusion

A CO_2 laser can rapidly change the temperature of solution inside the tip of a borosilicate glass electrospray emitter. A change in laser power from zero (ambient temperature) to 1.2 W results in a steady state solution temperature of 78 °C within less than 0.5 s. The fast heating time is a result of high absorption of borosilicate and the low thermal mass of the emitter tip that enables rapid energy transfer into the aqueous solution. The time necessary to return from a steady state temperature of 83 °C to ambient temperature after turning off the laser is about four seconds. The longer time for cooling reflects the slow thermal transfer rate from the tip of the capillary to the rest of the capillary as well as to the surrounding air, which could be improved by forced air cooling. Heating and cooling with LH-ESI is more than 100x faster than a thermally heated apparatus that was constructed for comparison.

This high heating/cooling rate makes it possible to acquire data as a function of laser power at least 31 times quicker than a conventional vT-ESI device. Laser powers can be calibrated to solution temperatures using the melting curves of proteins measured with both LH-ESI and vT-ESI. This calibration works well for proteins that have similar melting temperatures as the calibrant, but is most sensitive where there is the greatest change in the average charge with temperature. The ideal laser power-temperature calibrant would have a steady change in the average charge state over a large temperature range and would not undergo aggregation or degradation. An advantage of using a laser to heat the emitter tip vs heating nanodroplets directly is that >2000x lower laser fluence can be used. The laser power needed for LH-ESI could be reduced by focusing the laser at the emitter tip and should enable low powered lasers to be used in these experiments. Alternative wavelengths, such as 2.9 μm, which is the maximum

in the absorption for liquid water in the infrared region, could mitigate the power differences in heating the emitter vs. the droplets directly.

LH-ESI shows significant promise for coupling with separation techniques. Native capillary electrophoretic separations often have peak widths <1 minute, which is less than the typical thermal equilibration time in vT-ESI. In contrast, an entire melting curve could be acquired with LH-ESI within this time. These thermal stability measurements would add an extra dimension of information to native MS coupled to separations. Rapidly heating just the end of the borosilicate emitter also has the potential to mitigate aggregation processes that occur above the T_m of a protein, which can be an issue with vT-ESI due to the significantly longer measurement times at high temperature. As a result of the quick thermal equilibration, LH-ESI may enable the analysis of the thermal stability of aggregation-prone proteins above the T_m before oligomerization disrupts the electrospray process. Protein desalting using submicron borosilicate emitters has enabled the study of protein structures from biochemically relevant buffers.[53,54] LH-ESI with submicron emitters could potentially be used for high-throughput thermal stability screens of proteins, macromolecular complexes, and antibodies directly from formulation buffers, quickly identifying candidates for further investigation during the development of novel biotherapeutics.

Supporting Information: Effect of emitter position on cyt *c* melting during LH-ESI; vT-ESI apparatus thermal equilibration time measurement; Laser-power to solution temperature calibration and example calibration curve.

Acknowledgements

The authors thank Dr. Anthony T. Iavarone and Dr. Conner C. Harper for insightful discussions, Dr. Sanjay R. Krishnaswamy for sample preparation of pseudo-wild type barstar and reviewers for their helpful comments and suggestions. This material is based upon work supported by the National Science Foundation Division of Chemistry under grant number CHE-1609866, CHE-2203907, a Graduate Research Fellowship (DGE-2146752), CALSOLV, as well as the Merck DBL SEEDS program. The authors thank the staff at the University of California, Berkeley Electron Microscopy Laboratory for advice on electrospray emitter imaging.

References

(1) Ibarra-Molero, B.; Loladze, V. V.; Makhatadze, G. I.; Sanchez-Ruiz, J. M. Thermal versus Guanidine-Induced Unfolding of Ubiquitin. An Analysis in Terms of the Contributions from Charge-Charge Interactions to Protein Stability. *Biochemistry* **1999**, *38*, 8138–8149.

(2) Norma J. Greenfield. Using Circular Dichroism Collected as a Function of Temperature to Determine the Thermodynamics of Protein Unfolding and Binding Interactions. *Nat. Protoc.* **2006**, *1*, 2527–2535.

(3) Huynh, K.; Partch, C. L. Analysis of Protein Stability and Ligand Interactions by Thermal Shift Assay. *Curr. Protoc. Protein Sci.* **2015**, *79*, 28.9.1-28.9.14.

(4) Schultz, D. A.; Baldwin, R. L. Cis Proline Mutants of Ribonuclease A. I. Thermal Stability. *Protein Sci.* **1992**, *1*, 910–916.

(5) Shih, P.; Kirsch, J. F.; Holland, D. R. Thermal Stability Determinants of Chicken Egg-White Lysozyme Core Mutants: Hydrophobicity, Packing Volume, and Conserved Buried Water Molecules. *Protein Sci.* **1995**, *4*, 2050–2062.

(6) Marchand, A.; Rosu, F.; Zenobi, R.; Gabelica, V. Thermal Denaturation of DNA G-

Quadruplexes and Their Complexes with Ligands: Thermodynamic Analysis of the Multiple States Revealed by Mass Spectrometry. *J. Am. Chem. Soc.* **2018**, *140*, 12553–12565.

(7) Lo, M. C.; Aulabaugh, A.; Jin, G.; Cowling, R.; Bard, J.; Malamas, M.; Ellestad, G. Evaluation of Fluorescence-Based Thermal Shift Assays for Hit Identification in Drug Discovery. *Anal. Biochem.* **2004**, *332*, 153–159.

(8) Harrison, J. A.; Pruška, A.; Oganesyan, I.; Bittner, P.; Zenobi, R. Temperature-Controlled Electrospray Ionization: Recent Progress and Applications. *Chem. Eur. J.* **2021**, *27*, 18015–18028.

(9) Wen, J.; Lord, H.; Knutson, N.; Wikström, M. Nano Differential Scanning Fluorimetry for Comparability Studies of Therapeutic Proteins. *Anal. Biochem.* **2020**, *593*, 113581.

(10) Poklar, N.; Vesnaver, G. Thermal Denaturation of Proteins Studied by UV Spectroscopy. *J. Chem. Educ.* **2000**, *77*, 380.

(11) Kresheck, G. C.; Erman, J. E. Calorimetric Studies of the Thermal Denaturation of Cytochrome c Peroxidase. *Biochemistry* **1988**, *27*, 2490–2496.

(12) Wang, G.; Bondarenko, P. V.; Kaltashov, I. A. Multi-Step Conformational Transitions in Heat-Treated Protein Therapeutics Can Be Monitored in Real Time with Temperature-Controlled Electrospray Ionization Mass Spectrometry. *Analyst* **2018**, *143*, 670–677.

(13) Jarzab, A.; Kurzawa, N.; Hopf, T.; Moerch, M.; Zecha, J.; Leijten, N.; Bian, Y.; Musiol, E.; Maschberger, M.; Stoehr, G.; Becher, I.; Daly, C.; Samaras, P.; Mergner, J.; Spanier, B.; Angelov, A.; Werner, T.; Bantscheff, M.; Wilhelm, M.; Klingenspor, M.; Lemeer, S.; Liebl, W.; Hahne, H.; Savitski, M. M.; Kuster, B. Meltome Atlas—Thermal Proteome Stability across the Tree of Life. *Nat. Methods* **2020**, *17*, 495–503.

(14) Vallejo, D. D.; Rojas Ramírez, C.; Parson, K. F.; Han, Y.; Gadkari, V. V.; Ruotolo, B. T. Mass Spectrometry Methods for Measuring Protein Stability. *Chem. Rev.* **2022**, *122*, 7690–7719.

(15) El-Baba, T. J.; Fuller, D. R.; Woodall, D. W.; Raab, S. A.; Conant, C. R.; Dilger, J. M.; Toker, Y.; Williams, E. R.; Russell, D. H.; Clemmer, D. E. Melting Proteins Confined in Nanodroplets with 10.6 μm Light Provides Clues about Early Steps of Denaturation. *Chem. Commun.* **2018**, *54*, 3270–3273.

(16) Wyttenbach, T.; Bowers, M. T. Structural Stability from Solution to the Gas Phase: Native Solution Structure of Ubiquitin Survives Analysis in a Solvent-Free Ion Mobility-Mass Spectrometry Environment. *J. Phys. Chem. B* **2011**, *115*, 12266–12275.

(17) Gross, D. S.; Zhao, Y.; Williams, E. R. Dissociation of Heme-Globin Complexes by Blackbody Infrared Radiative Dissociation: Molecular Specificity in the Gas Phase? *J. Am. Soc. Mass Spectrom.* **1997**, *8*, 519–524.

(18) Brown, C. J.; Woodall, D. W.; El-Baba, T. J.; Clemmer, D. E. Characterizing Thermal Transitions of IgG with Mass Spectrometry. *J. Am. Soc. Mass Spectrom.* **2019**, *30*, 2438–2445.

(19) El-Baba, T. J.; Raab, S. A.; Buckley, R. P.; Brown, C. J.; Lutomski, C. A.; Henderson, L. W.; Woodall, D. W.; Shen, J.; Trinidad, J. C.; Niu, H.; Jarrold, M. F.; Russell, D. H.; Laganowsky, A.; Clemmer, D. E. Thermal Analysis of a Mixture of Ribosomal Proteins by vT-ESI-MS: Toward a Parallel Approach for Characterizing the Stabilitome. *Anal. Chem.* **2021**, *93*, 8484–8492.

(20) El-Baba, T. J.; Woodall, D. W.; Raab, S. A.; Fuller, D. R.; Laganowsky, A.; Russell, D. H.; Clemmer, D. E. Melting Proteins: Evidence for Multiple Stable Structures upon

Thermal Denaturation of Native Ubiquitin from Ion Mobility Spectrometry-Mass Spectrometry Measurements. *J. Am. Chem. Soc.* **2017**, *139*, 6306–6309.

(21) Woodall, D. W.; Henderson, L. W.; Raab, S. A.; Honma, K.; Clemmer, D. E. Understanding the Thermal Denaturation of Myoglobin with IMS-MS: Evidence for Multiple Stable Structures and Trapped Pre-Equilibrium States. *J. Am. Soc. Mass Spectrom.* **2021**, *32*, 64–72.

(22) Woodall, D. W.; El-Baba, T. J.; Fuller, D. R.; Liu, W.; Brown, C. J.; Laganowsky, A.; Russell, D. H.; Clemmer, D. E. Variable-Temperature ESI-IMS-MS Analysis of Myohemerythrin Reveals Ligand Losses, Unfolding, and a Non-Native Disulfide Bond. *Anal. Chem.* **2019**, *91*, 6808–6814.

(23) El-Baba, T. J.; Clemmer, D. E. Solution Thermochemistry of Concanavalin A Tetramer Conformers Measured by Variable-Temperature ESI-IMS-MS. *Int. J. Mass Spectrom.* **2019**, *443*, 93–100.

(24) Benesch, J. L. P.; Sobott, F.; Robinson, C. V. Thermal Dissociation of Multimeric Protein Complexes by Using Nanoelectrospray Mass Spectrometry. *Anal. Chem.* **2003**, *75*, 2208–2214.

(25) Wang, G.; Abzalimov, R. R.; Kaltashov, I. A. Direct Monitoring of Heat-Stressed Biopolymers with Temperature-Controlled Electrospray Ionization Mass Spectrometry. *Anal. Chem.* **2011**, *83*, 2870–2876.

(26) Shirzadeh, M.; Poltash, M. L.; Laganowsky, A.; Russell, D. H. Structural Analysis of the Effect of a Dual-FLAG Tag on Transthyretin. *Biochemistry* **2020**, *59*, 1013–1022.

(27) Jeanne Dit Fouque, K.; Fernandez-Lima, F. Following Structural Changes by Thermal Denaturation Using Trapped Ion Mobility Spectrometry-Mass Spectrometry. *J. Phys.*

Chem. B **2020**, *124*, 6257–6265.

(28) Geels, R. B. J.; Calmat, S.; Heck, A. J. R.; van der Vies, S. M.; Heeren, R. M. A. Thermal Activation of the Co-Chaperonins GroES and Gp31 Probed by Mass Spectrometry. *Rapid Commun. Mass Spectrom.* **2008**, *22*, 3633–3641.

(29) Harrison, J. A.; Pruška, A.; Bittner, P.; Muck, A.; Cooper-Shepherd, D. A.; Zenobi, R. Advancing Cyclic Ion Mobility Mass Spectrometry Methods for Studying Biomolecules: Toward the Conformational Dynamics of Mega Dalton Protein Aggregates. *Anal. Chem.* **2022**, *94*, 12435–12443.

(30) Kostelic, M. M.; Ryan, J. P.; Brown, L. S.; Jackson, T. W.; Hsieh, C.; Zak, C. K.; Sanders, H. M.; Liu, Y.; Chen, V. S.; Byrne, M.; Aspinwall, C. A.; Baker, E. S.; Marty, M. T. Stability and Dissociation of Adeno-Associated Viral Capsids by Variable Temperature-Charge Detection-Mass Spectrometry. *Anal. Chem.* **2022**, *94*, 11723–11727.

(31) Marchand, A.; Czar, M. F.; Eggel, E. N.; Kaeslin, J.; Zenobi, R. Studying Biomolecular Folding and Binding Using Temperature-Jump Mass Spectrometry. *Nat. Commun.* **2020**, *11*, 566.

(32) Cong, X.; Liu, Y.; Liu, W.; Liang, X.; Russell, D. H.; Laganowsky, A. Determining Membrane Protein-Lipid Binding Thermodynamics Using Native Mass Spectrometry. *J. Am. Chem. Soc.* **2016**, *138*, 4346–4349.

(33) Qiao, P.; Schrecke, S.; Walker, T.; McCabe, J. W.; Lyu, J.; Zhu, Y.; Zhang, T.; Kumar, S.; Clemmer, D.; Russell, D. H.; Laganowsky, A. Entropy in the Molecular Recognition of Membrane Protein-Lipid Interactions. *J. Phys. Chem. Lett.* **2021**, *12*, 12218–12224.

(34) Raab, S. A.; El-Baba, T. J.; Woodall, D. W.; Liu, W.; Liu, Y.; Baird, Z.; Hales, D. A.; Laganowsky, A.; Russell, D. H.; Clemmer, D. E. Evidence for Many Unique Solution

Structures for Chymotrypsin Inhibitor 2: A Thermodynamic Perspective Derived from vT-ESI-IMS-MS Measurements. *J. Am. Chem. Soc.* **2020**, *142*, 17372–17383.

(35) Pruška, A.; Marchand, A.; Zenobi, R. Novel Insight into Proximal DNA Domain Interactions from Temperature-Controlled Electrospray Ionization Mass Spectrometry. *Angew. Chemie Int. Ed.* **2021**, *60*, 15390–15398.

(36) McCabe, J. W.; Shirzadeh, M.; Walker, T. E.; Lin, C. W.; Jones, B. J.; Wysocki, V. H.; Barondeau, D. P.; Clemmer, D. E.; Laganowsky, A.; Russell, D. H. Variable-Temperature Electrospray Ionization for Temperature-Dependent Folding/Refolding Reactions of Proteins and Ligand Binding. *Anal. Chem.* **2021**, *93*, 6924–6931.

(37) Walker, T. E.; Shirzadeh, M.; Sun, H. M.; McCabe, J. W.; Roth, A.; Moghadamchargari, Z.; Clemmer, D. E.; Laganowsky, A.; Rye, H.; Russell, D. H. Temperature Regulates Stability, Ligand Binding (Mg^{2+} and ATP), and Stoichiometry of GroEL-GroES Complexes. *J. Am. Chem. Soc.* **2022**, *144*, 2667–2678.

(38) Shi, X.; Takamizawa, A.; Nishimura, Y.; Hiraoka, K.; Akashi, S. Thermal Unfolding of Proteins Probed by Laser Spray Mass Spectrometry. *Rapid Commun. Mass Spectrom.* **2008**, *22*, 1430–1436.

(39) Nakamura, M.; Takamizawa, A.; Yamada, H.; Hiraoka, K.; Akashi, S. Denaturation of α-Lactalbumin and Ubiquitin Studied by Electrospray and Laser Spray. *Rapid Commun. Mass Spectrom.* **2007**, *21*, 1635–1643.

(40) Hiraoka, K.; Saito, S.; Katsuragawa, J.; Kudaka, I. A New Liquid Chromatography/Mass Spectrometry Interface: Laser Spray. *Rapid Commun. Mass Spectrom.* **1998**, *12*, 1170–1174.

(41) Kudaka, I.; Kojima, T.; Saito, S.; Hiraoka, K. A Comparative Study of Laser Spray and

Electrospray. *Rapid Commun. Mass Spectrom.* **2000**, *14*, 1558–1562.

(42) Hiraoka, K. Laser Spray: Electric Field-Assisted Matrix-Assisted Laser Desorption/Ionization. *J. Mass Spectrom.* **2004**, *39*, 341–350.

(43) Takamizawa, A.; Itoh, Y.; Osawa, R.; Iwasaki, N.; Nishimura, Y.; Akashi, S.; Hiraoka, K. Selective Dissociation of Non-Covalent Bonds in Biological Molecules by Laser Spray. *J. Mass Spectrom.* **2004**, *39*, 1053–1058.

(44) Shi, X.; Nishimura, Y.; Akashi, S.; Takamizawa, A.; Hiraoka, K. Evaluation of Binding Affinity of Protein-Mutant DNA Complexes in Solution by Laser Spray Mass Spectrometry. *J. Am. Soc. Mass Spectrom.* **2006**, *17*, 611–620.

(45) Shi, X.; Takamizawa, A.; Nishimura, Y.; Hiraoka, K.; Akashi, S. Stability Analysis for Double-Stranded DNA Oligomers and Their Noncovalent Complexes with Drugs by Laser Spray. *J. Mass Spectrom.* **2006**, *41*, 1086–1095.

(46) Mortensen, D. N.; Williams, E. R. Ultrafast (1 μs) Mixing and Fast Protein Folding in Nanodrops Monitored by Mass Spectrometry. *J. Am. Chem. Soc.* **2016**, *138*, 3453–3460.

(47) Mortensen, D. N.; Williams, E. R. Investigating Protein Folding and Unfolding in Electrospray Nanodrops upon Rapid Mixing Using Theta-Glass Emitters. *Anal. Chem.* **2015**, *87*, 1281–1287.

(48) Mortensen, D. N.; Williams, E. R. Theta-Glass Capillaries in Electrospray Ionization: Rapid Mixing and Short Droplet Lifetimes. *Anal. Chem.* **2014**, *86*, 9315–9321.

(49) Xia, Z.; Williams, E. R. Effect of Droplet Lifetime on Where Ions Are Formed in Electrospray Ionization. *Analyst* **2019**, *144*, 237–248.

(50) Jordan, J. S.; Xia, Z.; Williams, E. R. Tips on Making Tiny Tips: Secrets to Submicron Nanoelectrospray Emitters. *J. Am. Soc. Mass Spectrom.* **2022**, *33*, 607–611.

(51) Sterling, H. J.; Williams, E. R. Origin of Supercharging in Electrospray Ionization of Noncovalent Complexes from Aqueous Solution. *J. Am. Soc. Mass Spectrom.* **2009**, *20*, 1933–1943.

(52) Krishnaswamy, S. R.; Williams, E. R.; Kirsch, J. F. Free Energies of Protein-Protein Association Determined by Electrospray Ionization Mass Spectrometry Correlate Accurately with Values Obtained by Solution Methods. *Protein Sci.* **2006**, *15*, 1465–1475.

(53) Susa, A. C.; Xia, Z.; Williams, E. R. Small Emitter Tips for Native Mass Spectrometry of Proteins and Protein Complexes from Nonvolatile Buffers That Mimic the Intracellular Environment. *Anal. Chem.* **2017**, *89*, 3116–3122.

(54) Susa, A. C.; Xia, Z.; Williams, E. R. Native Mass Spectrometry from Common Buffers with Salts That Mimic the Extracellular Environment. *Angew. Chemie Int. Ed.* **2017**, *56*, 7912–7915.

(55) Sahba, N.; Rockett, T. J. Infrared Absorption Coefficients of Silica Glasses. *J. Am. Ceram. Soc.* **1992**, *75*, 209–212.

(56) Yang, F.; Zhou, B. R.; Zhang, P.; Zhao, Y. F.; Chen, J.; Liang, Y. Binding of Ferulic Acid to Cytochrome c Enhances Stability of the Protein at Physiological PH and Inhibits Cytochrome C-Induced Apoptosis. *Chem. Biol. Interact.* **2007**, *170*, 231–243.

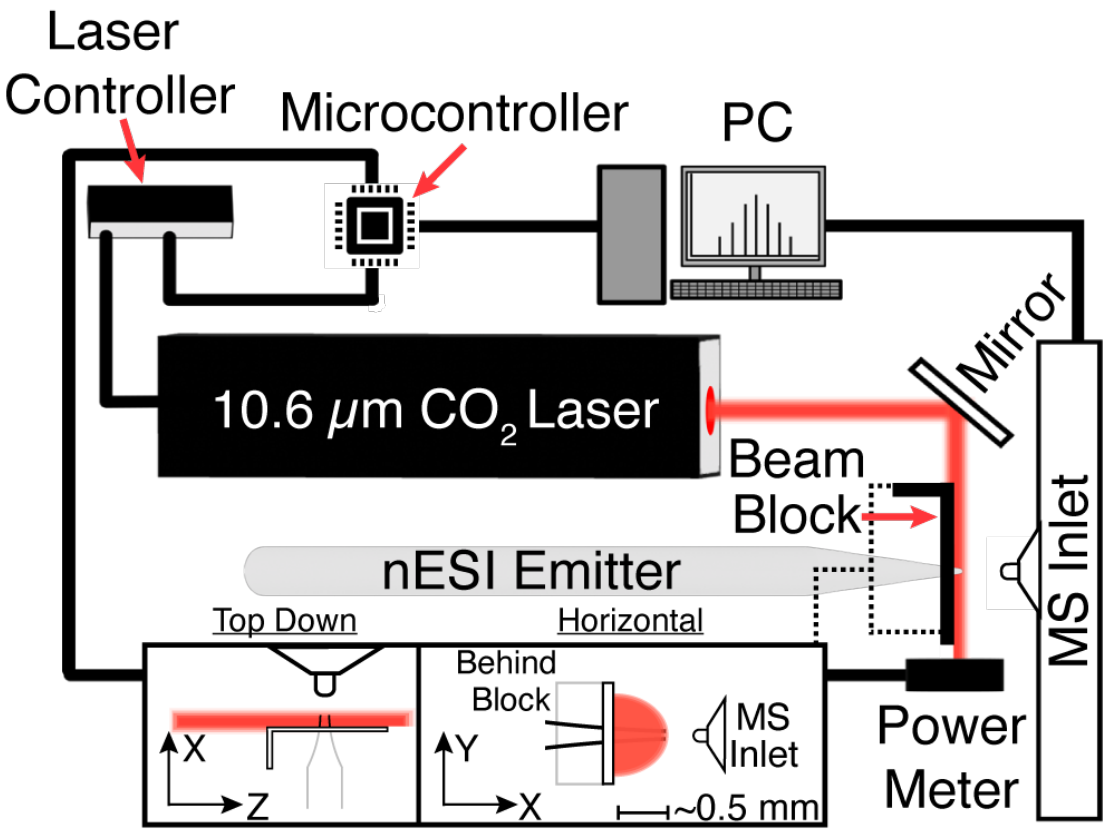

Figure 1. A schematic diagram of the laser heating device in combination with a mass spectrometer, where the tip of a borosilicate capillary is irradiated with 10.6 μm light from an unfocused CO_2 laser and laser power was measured and controlled with a microcontroller. The inset shows the emitter passing through the beam block.

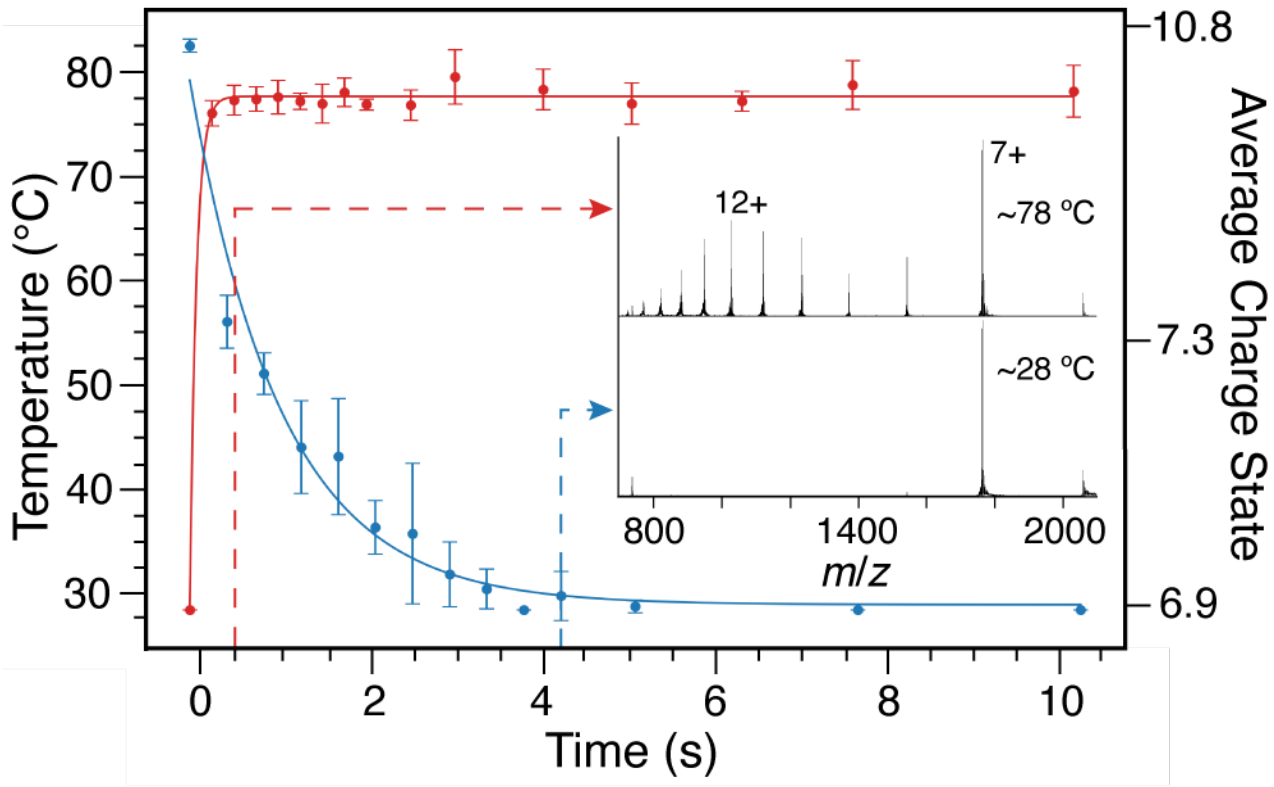

Figure 2. The average charge state of cyt *c* (right *y*-axis) as a function of time after the laser is turned on at a power of 1.2 W (red data) and after the laser is turned off at a marginally higher laser power (blue data). The inset shows mass spectra acquired 0.5 s after turning the laser on (top) and 4.2 s after turning the laser off (bottom). These data are converted to temperature (left *y*-axis) using the method described in the text. A blank spectrum shows that the peak at m/z = 711 is a contaminant.

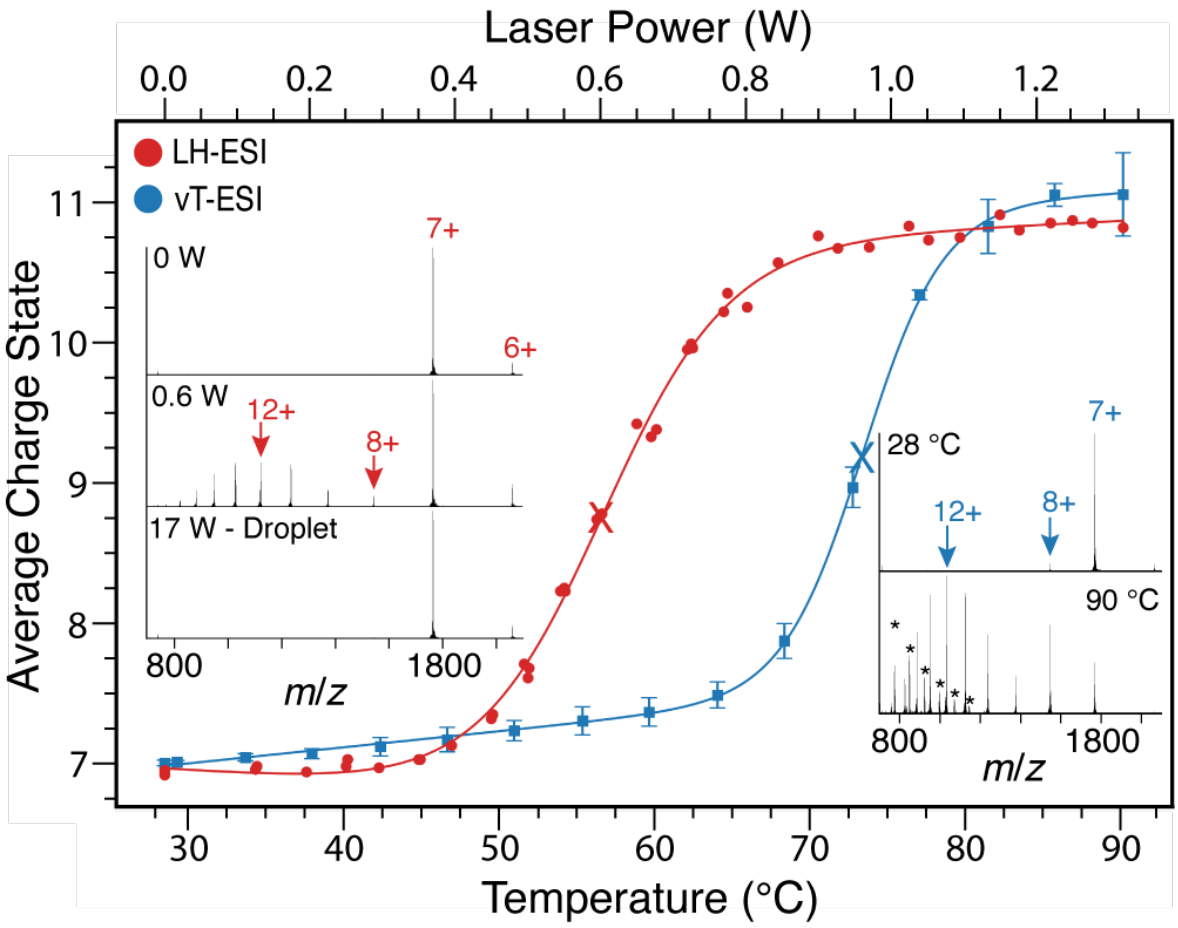

Figure 3. Melting curves for cyt *c* obtained by LH-ESI (red) and vT-ESI (blue). Data points from LH-ESI replicates are not typically at exactly the same laser power due to slight variations in laser power. A melting temperature and melting power of 73.5 ± 0.5 °C (blue cross) and 0.599 ± 0.001 W (red cross) are obtained from sigmoidal fits to the resistively heated and laser-heated data, respectively. Mass spectra of cyt *c* (left inset) acquired by emitter heating (middle) show a distribution at lower *m*/*z* indicating substantial protein unfolding at this power, but nanodroplet heating with a beam focused to ~1 mm (bottom) shows no evidence of protein unfolding. The right inset shows mass spectra acquired at different solution temperatures by vT-ESI. Asterisks indicate PDMS contaminant peaks.

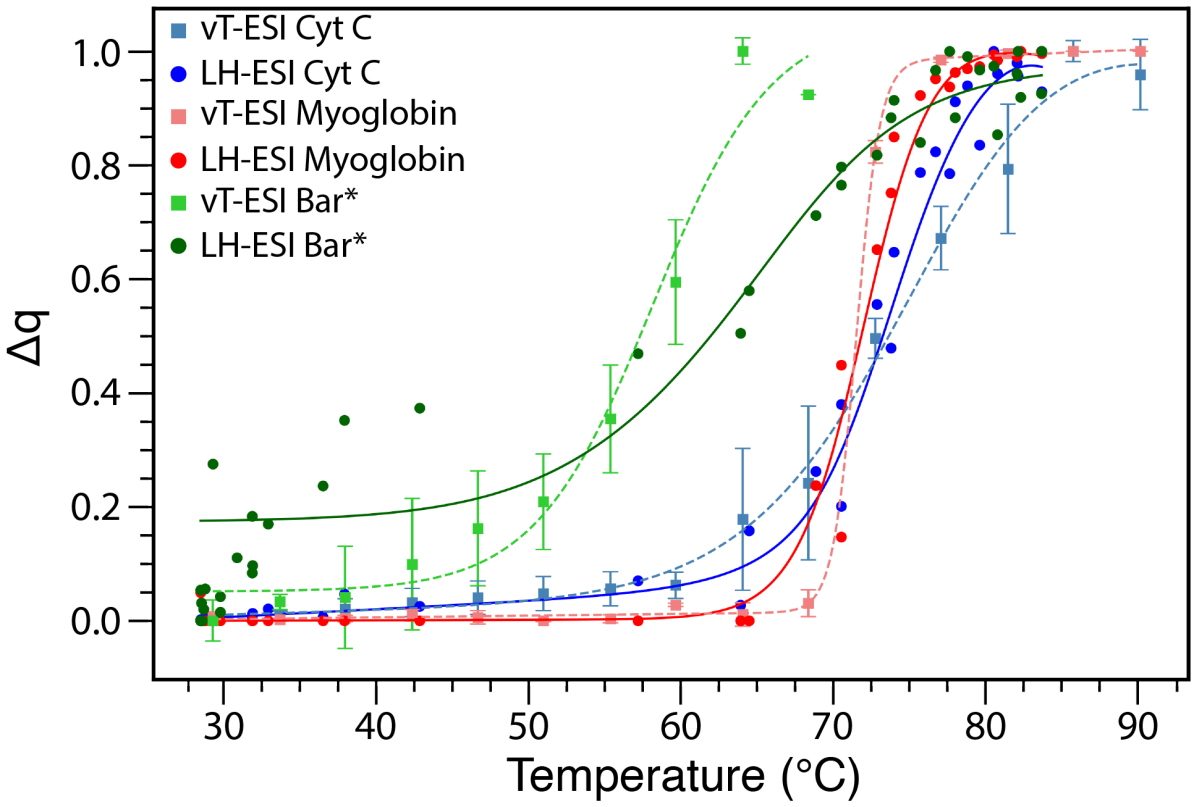

Figure 4. Temperature-calibrated melting curves for cyt *c*, myoglobin, and Ψbar* from LH-ESI (solid curves) and vT-ESI (dashed curves). The melting temperatures determined for myoglobin and Ψbar* from LH-ESI experiments agree with those obtained from vT-ESI.

TOC Graphic

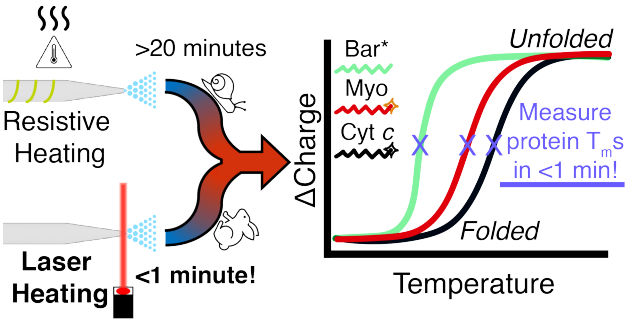
>20 minutes
Resistive Heating
Laser Heating
<1 minute!
Bar*
Myo
Cyt c
ΔCharge
Unfolded
Folded
Measure protein T_ms in <1 min!
Temperature